Current **A**pplied **S**cience and **T**echnology e-ISSN: 2586-9396

Curr. Appl. Sci. Technol. 2025, Vol. 25 (No. 4), e0262003

Research article

Antioxidant Activity and Anti-tyrosinase Activity of *Nelumbo nucifera* Gaertn. Flower Extract Encapsulated in Layered Double Hydroxide

Jayani C. Dhanasinghe, Nadun S. Ubeysinghe and Ireshika C. De Silva*

Department of Chemistry, Faculty of Science, University of Colombo, Colombo 03 110001, Sri Lanka

Received: 28 January 2024 , Revised: 24 October 2024, Accepted: 17 November 2024, Published: 28 January 2025

Abstract

Dermatological problem is mainly caused by reactive oxygen species (ROS) and excessive tyrosinase level in human body. It becomes interesting in the field of biological research which has been attempted to develop new materials from plant extracts to solve this problem. The concern is how those components in the plant extract can be used, protected, and released efficiently during application processes. In this study, we aimed to create a layered double hydroxide (LDH) encapsulating white lotus (*Nelumbo nucifera* Gaertn.) flower extract (WLE-LDH), investigate the antioxidant and anti-tyrosinase effects of *Nelumbo nucifera* Gaertn. flower extract encapsulated in the layered double hydroxide (WLE-LDH), and assess the release properties of the nanohybrid. DPPH assay and anti-tyrosinase enzyme assay were performed on methanol extract of *N. nucifera* and WLE-LDH. The white lotus methanolic extract demonstrated antioxidant activity with an EC_{50} of 0.17 mg mL^{-1} and uncompetitive inhibition of tyrosinase with an IC_{50} of 0.43 mg mL^{-1}. The reconstruction method was used to encapsulate the white lotus flower extract into Mg-Al LDH without isolating the phytochemicals. The successful intercalation of the crude flower extract into the layered structure was confirmed by an increase in the interlayer spacing as indicated by shift in the powder X-ray diffraction pattern. Fourier transform infrared spectroscopy data and SEM image also showed that an encapsulated nanohybrid had been successfully formed. Further, the data of exposure to ultraviolet–visible light suggested that the crude extract of *N. nucifera* Gaertn. flower was stabilized within the LDH bilayer, protecting its bioactivities. The resulting nanohybrid with bioactive phytoconstituents showed antioxidant activity with an EC_{50} of 0.58 mg mL^{-1} and anti-tyrosinase activity with an IC_{50} of 0.63 mg mL^{-1}. Furthermore, the WLE-LDH sample demonstrated slow and controlled release characteristics with antioxidant activity for up to 3½ h and anti-tyrosinase activity for up to 2½ h. Our findings suggest a promising strategy of its potential applications in the cosmetic and pharmaceutical industries.

Keywords: *Nelumbo nucifera* Gaertn; flower extract; layered double hydroxide; WLE-LDH; antioxidant activity; anti-tyrosinase activity

*Corresponding author: E-mail: hicdesilva@chem.cmb.ac.lk
https://doi.org/10.55003/cast.2025.262003

1. Introduction

The use of natural sources for production of pharmaceuticals has gained significant attention due to the discovery of the healing properties of plant-based therapies in conventional medicine (Sasidharan et al., 2011; Megalathan et al., 2016). Multiple efforts have been made in this regard to incorporate traditional medicines with western pharmacological compositions. There is a growing interest in natural biomolecules even with the widely recognized difficulties in turning them into powerful medicines. This has led to extensive interdisciplinary research for plant-based drug discovery (Megalathan et al., 2016). Formulations based on plant materials and extracts are becoming more popular globally owing to their low or zero toxicity, complete biodegradability, and in most instances, their easy fabrication when compared to materials produced by complete chemical processing (Tringali, 2001). Every part of the *Nelumbo nucifera* plant has medicinal value in various systems of medicine such as traditional, popular, and Ayurvedic medicine (Mukherjee et al., 2009). Among the traditional medicinal plants, *Nelumbo nucifera* Gaertn. flowers are known to have various therapeutic properties, including antioxidant (Gunawardana & Jayasuriya, 2019) and anti-tyrosinase (Kim et al., 2011) activity. The most important classes of compounds discovered in the flowers of *N. nucifera* Gaertn. are alkaloids, carbohydrates, terpenoids, saponins, tannins, flavonoids, glycosides, and polyphenols (Mukherjee et al., 2009; Subasini et al., 2014; Dubey & Baghel, 2019). Out of many common health related issues, skin photoaging, oxidative stress-induced inflammation that increases pigmentation, DNA damage caused by reactive oxygen species in the skin, and melanin overproduction induced skin-related disorders (Chen et al., 2021) represent a significant burden to the healthcare systems. *Nelumbo nucifera* Gaertn. flower extract would be a possible candidate for the therapy of such skin disorders.

Due to poor bioavailability, low stability, and low water solubility, *N. nucifera* Gaertn. flower extract phytochemicals have limited practical applications. As a result, it is necessary to modify the qualities of the plant extract phytochemicals to create a diverse, practical, and efficient medicinal product. The pharmaceutical sector has gained tremendous opportunities from nanotechnology (Karunaratne et al., 2012). The ability of nanolayered inorganic materials to encapsulate and immobilize a variety of organic and inorganic molecules as well as biomolecules in the interlayer space has drawn a great deal of attention among many different types of nanomaterials that are currently available. This is because of the fascinating lamellar structures of nanolayered inorganic materials (Alcântara et al., 2010). The application of layered double hydroxides as drug delivery vehicles has attracted significant interest owing to their potential benefits such as protecting incorporated plant extracts from harsh environment conditions, controlling the release of therapeutic components, the structural and morphological tunability, convenient synthesis, versatility, low toxicity, good biocompatibility, bio-degradability and facilitating drug delivery into the target cell (Daniel & Thomas, 2020). Layered double hydroxides (LDHs) are two-dimensional inorganic layered nanomaterials which can be either natural or synthetic. They have the common formula of $[M(II)_{1-x}M(III)_x(OH)_2]^{x+}[A^{n-}_{x/n}.nH_2O]^{x-}$. In this formula, M(II) is a divalent metal cation, M(III) is a trivalent metal cation, A is an exchangeable anion, n is the number of water moles, and x is the M(III)/[M(II) + M(III)] molar ratio, usually in the range of $0.1 \leq x \leq 0.5$ (Eckelt et al., 2009). The structure of LDHs contains positively charged mixed metal hydroxide layers and exchangeable anions. The exchangeable anions balance the residual positive charges of the metal hydroxide layer (Daniel & Thomas, 2020).

LDH-based drug delivery systems have the potential to encapsulate naturally occurring biologically active molecules within the layered structures of their LDH nanolayers. Earlier studies have reported some work on these systems which were used for controlled- and slow-release applications. Samindra & Kottegoda (2014) attempted to stabilize curcumin molecules within LDH nanolayers using a simple *in-situ* co-precipitation method. The prevention of degradation and slow release of curcumin from the curcumin intercalated LDH was demonstrated. The outcomes indicated the positive potential of intercalated LDH in therapeutic applications (Samindra & Kottegoda, 2014). Later studies were conducted to test the therapeutic potential of curcuminoids-LDH. The resulting LDH showed significant antimicrobial activity against three bacterial and two fungal species while showing consistent and slow release of curcuminoids from the nanohybrid in an acidic medium (Megalathan et al., 2016). Citrate ions were incorporated into the layers of Mg-Al LDH. The resulting citrate LDH was then properly incorporated into a cocoa-butter-containing body cream formulation. The citrate LDH and the nanohybrid body formulation showed prolonged slow release of citrate ions at acidic pH values. They also showed activity against *Candida species* (Perera et al., 2015). Shafiei *et al.* (2015) described the efficient encapsulation of epigallocatechin gallate into a layered double hydroxide and its *in vitro* anti-tumor properties. Kim *et al.* (2016) reported the formation of a nanohybrid using both root and flower extracts of AGN (*Angelica gigas* Nakai.) into LDH. In the later expanded study, AGN-LDH hybrids were evaluated for their anticancer activity (Kim et al., 2018). Kim *et al.* (2019) also reported the successful intercalation of *Zingiber officinale* extract (ZOE) into LDH and demonstrated its antioxidant activity while preserving the *Zingiber officinale* extract from external damage from ultrasound and microwave irradiation. In recent literature, Perotti *et al.* (2020) reported the successful encapsulation of Norbixin isolated from *Bixa orellana* L. (annatto) extract into layered double hydroxide and its radical scavenging activity. In addition, Jeung et al. (2019) synthesized *Glycine max* Merrill (GM) extract incorporated LDHs using ion exchange and reconstruction methods and studied the alkaline phosphatase activity of the resulting nanohybrids.

Herein, we report an effective synthesis of naturally extracted *N. nucifera* Gaertn. flower extract incorporated into layered double hydroxide nanohybrids *via* the reconstruction approach. LDH plays a dual role by enhancing the stability of phytochemicals in *N. nucifera* Gaertn. flower extract and acting as a delivery vehicle for the slow, precise, and sustained release of the phytochemicals over a prolonged period. Moreover, the increased stability and moderate release of bioactive phytoconstituents in *Nelumbo nucifera* Gaertn. flower extract encapsulated LDH (WLE-LDH) nanohybrid exhibited excellent antioxidant and anti-tyrosinase properties.

2. Materials and Methods

2.1 Chemical and plant materials

Dimethyl sulfoxide (DMSO), hydrochloric acid (HCl), sodium hydroxide pellets (NaOH), mushroom tyrosinase, and 2,2-Diphenyl-1-picrylhydrazyl (DPPH) were purchased from Sigma-Aldrich. Magnesium nitrate hexahydrate ($Mg(NO_3)_2.6H_2O$) was purchased from Fujifilm Wako Pure Chemical Corporation. Sodium nitrate ($NaNO_3$) and L-tyrosine ($C_9H_{11}NO_3$) were purchased from Loba Chemie Pvt. Ltd. Aluminum nitrate nonahydrate ($Al(NO_3)_3.9H_2O$) and L-ascorbic acid (AA) were purchased from Himedia Laboratories. Disodium hydrogen orthophosphate (Na_2HPO_4) and sodium dihydrogen orthophosphate (NaH_2PO_4) were purchased from Daejung Chemicals & Metals Co., Ltd. Arbutin ($C_{12}H_{16}O_7$)

was purchased from Tokyo Chemical Industry Co., Ltd. All the chemicals and reagents used were of analytical grade and used without further purification. Methanol was double distilled prior to use. White lotus (*Nelumbo nucifera* Gaertn.) flowers were authenticated by Bandaranaike Memorial Ayurvedic Research Institute, Nawinna, Maharagama, Sri Lanka and deposited under accession number 3072.

2.2 Extraction of crude extract from *Nelumbo nucifera* Gaertn. flowers

A weight of 100 g of each of the petals, stamens, and stigmas of dried white lotus (*N. nucifera* Gaertn.) flowers were pulverized with a blender. A weight of 100 g of each flower part was split to 50 g, put into a 500 mL beaker, and then mixed with 250 mL of double-distilled methanol. Each mixture was sonicated (GRANT XUB10 model) at room temperature for 4 h with 100% power while swirling occasionally. Each extract was then allowed to stand in the dark for 30 min and then filtered with a muslin cloth. Each filtrate was collected into a 500 mL round bottom flask and evaporated using a rotary evaporator at 45ºC until a crude oily solution formed. Then, the crude product was transferred to an evaporating dish to remove the excess methanol in the mixture by heating at 70ºC on a heating mantle for 5 min (Jeon et al., 2009; Liyanaararchchi et al., 2018).

2.3 Synthesis of pristine Mg-Al layered double hydroxide (LDH)

The solutions of 50 mL of 1.0 M magnesium nitrate hexahydrate and 50 mL of 0.5 M aluminium nitrate nonahydrate were mixed in a beaker in a 2:1 ratio. Then, 60 mL of 0.5 M sodium nitrate was added to the reaction mixture. This was followed by dropwise addition of 2.0 M NaOH to the mixture while stirring at 1200 rpm with a magnetic stirrer until the pH reached 10. The solution mixture was stirred at 1200 rpm for 6 h at 60ºC while purging N_2. A white color creamy precipitate formed. The precipitate was filtered out by suction filtration, washed thoroughly with distilled water to remove impurities, and dried for 6 h at 90ºC in the oven (Samindra & Kottegoda, 2014). The dried white precipitate was powdered using a mortar and pestle. The white color powdered pristine LDH was kept at 4ºC (in a refrigerator) for further characterization.

2.4 Synthesis of encapsulated *Nelumbo nucifera* Gaertn. extract-layered double hydroxide (WLE-LDH)

A weight of 100 mg of *Nelumbo nucifera* Gaertn. extract was dissolved in 50 mL DMSO under vigorous stirring at 1200 rpm at room temperature in a round bottom flask. Then, 2 g of pristine Mg-Al LDH powder was added slowly to the concentrated mixture of 100 mg of *N. nucifera* Gaertn. flower extract in 50 mL of DMSO. The reaction mixture was stirred for 24 h at 1200 rpm at room temperature in dark conditions while purging N_2. The reaction mixture was kept in the dark for 12 h after stirring for 24 h until a solid appeared at the bottom of the round bottom flask. Then, the mixture was filtered by suction filtration and washed thoroughly with distilled water to remove impurities, and the dark-yellow colored precipitate (WLE-LDH) was collected in a crucible. The crucible with the collected sample was dried for 6 h at 90ºC in the oven (Samindra & Kottegoda, 2014; Megalathan et al., 2016). The encapsulated percentage of the flower extract was calculated using the following equation (1) (Megalathan et al., 2016).

$$Encapsulated\ percentage = \frac{Weight\ of\ lotus\ extract\ encapsulated\ into\ WLE-LDH}{Total\ weight\ of\ \ flower\ extract\ used} \times 100\ \% \qquad (1)$$

2.5 Characterization

Powder X-ray diffraction (PXRD) patterns of pristine Mg-Al LDH and WLE-LDH were taken to authenticate the formation of crystalline LDH solid by a Rigaku SmartLab SE powder X-ray diffractometer. The analysis was carried out using Cu Kα radiation at maximum wavelength 1.54059 Å over a 2θ angle from 0.0000° to 80.0000° with the step size of 0.20° (Poellmann & Witzke, 2010).

Fourier transform infrared (FTIR) spectra were recorded to identify the functional groups in the *N. nucifera* Gaertn. flower extract, pristine LDH, and WLE-LDH samples. A PerkinElmer Spectrum Two instrument was used to determine the functional groups in three different samples. Each powdered sample was placed on the disc and the measuring range was set up to 400 cm^{-1} to 4000 cm^{-1}.

Morphological study was carried out by scanning electron microscopy (SEM). SEM characterization was done using the ZEISS EVO scanning electron microscopy. The powdered samples were placed on gold coated slides and the scanning was done at nanometer range.

2.6 Antioxidant activity of WLE-LDH

2.6.1 2,2-Diphenyl-1-picrylhydrazyl (DPPH) free radical scavenging assay

The antioxidant activity of WLE-LDH composite was tested by using DPPH radical scavenging assay. WLE-LDH was tested at the assay concentration range of 0.0625-1 mg/mL. A volume of 100 µL of 152 µM DPPH solution was incubated with 100 µL of WLE-LDH dissolved in methanol at room temperature in the dark for 20 min. The absorbance was recorded against a blank at the wavelength of 520 nm for 1 h with 20 min intervals using a BIO-RAD Benchmark Plus microplate spectrophotometer. L-ascorbic acid was used as a positive standard (Tettey et al., 2012). The capacity to scavenge the DPPH radical by 50% (EC_{50}) was calculated from the dose effect curves by linear regression, and inhibition percentage was calculated using equation (2) (Liyanaararchchi et al., 2017).

$$Inhibition\ percentage = \frac{A_{Control} - A_{Sample}}{A_{Control}} \times 100\% \quad (2)$$

Where, A_{Sample} is the absorbance of the WLE-LDH sample, and $A_{Control}$ is the absorbance of the assay using methanol instead of the inhibitor (sample). The same procedure was followed for the standard solution series, control and for the white lotus flower extract solution series (Srichayanurak & Phadungkit, 2008).

2.6.2 Release behavior of WLE-LDH - antioxidant activity

To determine the release behavior of *N. nucifera* Gaertn. flower extract, the WLE-LDH (400 mg) was dissolved in 100 mL double-distilled methanol, in the dark. Then, the WLE-LDH mixture (2 mL) was added to a test tube with 2 mL of DPPH solution. The sample was incubated for 20 min in the dark at room temperature. The released amount of *N. nucifera* Gaertn. phytochemicals was determined at 5 min intervals by monitoring the variation of absorbance with a UV-Visible spectrophotometer until a constant absorbance value was obtained (Megalathan et al., 2016).

2.6.3 Determination of percentage of the extract released from WLE-LDH for antioxidant activity

To determine the released extract percentage of encapsulated *N. nucifera* Gaertn. extract from WLE-LDH, the WLE-LDH (400 mg) was dissolved in 100 mL of double-distilled methanol. Then, the WLE-LDH mixture (2 mL) was added to a test tube with 2 mL of DPPH solution. The sample was incubated for 20 min in the dark at room temperature. The absorbance was measured at 520 nm for 1 h with 20 min intervals using UV-Visible spectrophotometer. The released percentage was calculated using the following equation (3) (Megalathan et al., 2016).

$$Percentage\ released = \frac{Percentage\ of\ lotus\ flower\ extract\ release\ from\ WLE-LDH}{Concentration\ of\ lotus\ flower\ extract\ encapsulated} \times 100\% \quad (3)$$

2.7 Photo-stability study of *Nelumbo nucifera* Gaertn. flower extract and WLE-LDH for antioxidant action

Four 100 mg samples of WLE-LDH were exposed to UV light for 1, 2, 3, and 4 h. The samples were placed in a black box during the exposure. An equal weight of 10 mg of each WLE-LDH sample was measured and dissolved in a 10 mL volumetric flask using double-distilled methanol under dark conditions. Each sample of WLE-LDH (2 mL) was transferred to a test tube with nanoparticles. Then, 2 mL of DPPH solution was added to the test tube. Finally, the samples were incubated for 20 min in dark conditions at room temperature. An aliquot of each sample was placed in a glass cuvette and scanned from 200 nm to 900 nm using a GENESYS 180 UV-Visible spectrophotometer. The same procedure was repeated for the white lotus extract samples (Megalathan et al., 2016).

2.8 Anti-tyrosinase activity of WLE-LDH

2.8.1 Tyrosinase inhibition assay

The anti-tyrosinase activity of WLE-LDH composite was tested using a tyrosinase inhibition assay. A volume of 20 µL of WLE-LDH (varying concentrations from 0.0625-1 mg/mL), 20 µL of 50 units/mL mushroom tyrosinase aqueous solution, and 60 µL of 50 mM sodium phosphate buffer (pH 6.5) were mixed and pre-incubated at room temperature for 10 min. Then, 40 µL of 2 mM L-tyrosine was added. The mixture was then incubated for 30 min at room temperature. The amount of dopachrome was measured at the wavelength of 475 nm for 1 h with 10 min intervals using a BIO-RAD Benchmark Plus microplate spectrophotometer. Arbutin in sodium phosphate buffer was used as a positive standard. Sodium phosphate buffer (SPB) was used as the blank (Jeon et al., 2009; Tettey et al., 2012; Liyanaararchchi et al., 2017; Bakhouche et al., 2021). The capacity to inhibit tyrosinase by 50% (IC_{50}) was calculated from the dose effect curves by linear regression and inhibition percentage was calculated using following equation (4) (Liyanaararchchi et al., 2017).

$$Inhibition\ percentage = \frac{A_{Control} - A_{Sample}}{A_{Control}} \times 100\% \quad (4)$$

Where, A_{Sample} is the absorbance of the WLE-LDH sample, and $A_{Control}$ is the absorbance of the assay using the sodium phosphate buffer instead of inhibitor (sample).

The same procedure was followed for the standard solution series, control and for the *N. nucifera* Gaertn. flower extract solution series (Jeon et al., 2009; Tettey et al., 2012; Liyanaararchchi et al., 2017; Bakhouche et al., 2021).

2.8.2 Release behavior of WLE-LDH – anti-tyrosinase activity

To determine the release behavior of the encapsulated *N. nucifera* Gaertn. extract from WLE-LDH, 400 mg of the WLE-LDH was dissolved in 100 mL of double-distilled methanol. Then 0.5 mL of WLE-LDH mixture was added to a glass cuvette with 1.5 mL of SPB solution and 0.5 mL of enzyme solution. The sample was incubated for 10 min at room temperature. Finally, 1.0 mL of the substrate solution was added to the same glass cuvette. Here again, the sample was incubated for 30 min at room temperature. The amount of white lotus extract released from WLE-LDH was determined at 5 min intervals by monitoring the variation of absorbance at 475 nm in the UV-Visible spectrophotometer until a constant absorbance value was obtained (Megalathan et al., 2016).

2.8.3 Determination of percentage of the extract released from WLE-LDH for anti-tyrosinase activity

First, 400 mg of the WLE-LDH was dissolved in 100 mL of double-distilled methanol. Then 0.5 mL of the WLE-LDH mixture was added to a glass cuvette with 1.5 mL of SPB solution and 0.5 mL of tyrosinase enzyme solution. The sample was incubated for 10 min at room temperature. Finally, 1.0 mL of the substrate solution was added to the same glass cuvette. Then, the sample was incubated for 30 min at room temperature. The absorbance was measured at 475 nm for 1 h at 10 min intervals using a UV-Visible spectrophotometer. The released percentage was calculated using the following equation (5) (Megalathan et al., 2016).

$$Percentage\ released = \frac{Percentage\ of\ lotus\ flower\ extract\ release\ from\ WLE-LDH}{Concentration\ of\ lotus\ flower\ extract\ encapsulated} \times 100\% \quad (5)$$

2.9 Enzyme kinetics of *Nelumbo nucifera* Gaertn. extract

Various concentrations of L-tyrosine were used as substrates. A volume of 20 µL of 1 mg/mL *Nelumbo nucifera* Gaertn. flower extract, 20 µL of 50 units/mL mushroom tyrosinase aqueous solution, and 60 µL of 50 mM sodium phosphate buffer (pH 6.5) were mixed and pre-incubated at room temperature for 10 min. Then, 40 µL of L-tyrosine (varying concentrations from 3-0.5 mM) was added. Each mixture was then incubated for 30 min at room temperature. The amount of dopachrome was measured at the wavelength of 475 nm for at least 1 h at 5 min intervals using a BIO-RAD Benchmark Plus microplate spectrophotometer. The same procedure was followed for the control samples with the same concentrations of substrate solutions without adding 1.0 mg mL^{-1} *N. nucifera* Gaertn. flower extract solution. Here, SPB solution was used as the blank. The rate of the reaction was calculated using the following equation (6) (Crespo et al., 2019).

$$Rate\ of\ the\ reaction = \frac{Absorbance\ difference}{Time\ difference} \quad (6)$$

A Michaelis–Menten kinetic derivation was used to determine the kinetic parameters (Michaelis constant = K_m and maximum reaction velocity = V_{max}) and the type

of inhibition. Inhibitory kinetics of samples were analyzed *via* Lineweaver-Burk plots (Ashraf et al., 2015; Crespo et al., 2019).

3. Results and Discussion

The phytochemicals of *N. nucifera* Gaertn. flowers were extracted as a brown colored oily crude extract. The percentage yield of total phytoconstituents extracted from *N. nucifera* Gaertn. flower crude extract was 12.61% (w/w).

3.1 Characterization of Mg-Al layered double hydroxides (pristine LDH and WLE-LDH)

Solid-state characterization techniques such as powder X-ray diffraction (PXRD), Fourier transform infrared spectroscopy (FTIR), and scanning electron microscopy (SEM) were used to determine the successful encapsulation of *N. nucifera* Gaertn. flower extract into Mg-Al LDH.

3.2 X-ray diffraction study of the pristine Mg-Al LDH and WLE-LDH

The PXRD patterns (Figure 1) demonstrate the successful formation of the LDH nanostructures. The (003) reflection specific to the LDH structure was visible in both pristine LDH and WLE-LDH diffractograms. The results shown on the PXRD graph were in good agreement with the previously reported findings of the successful formation of LDH.

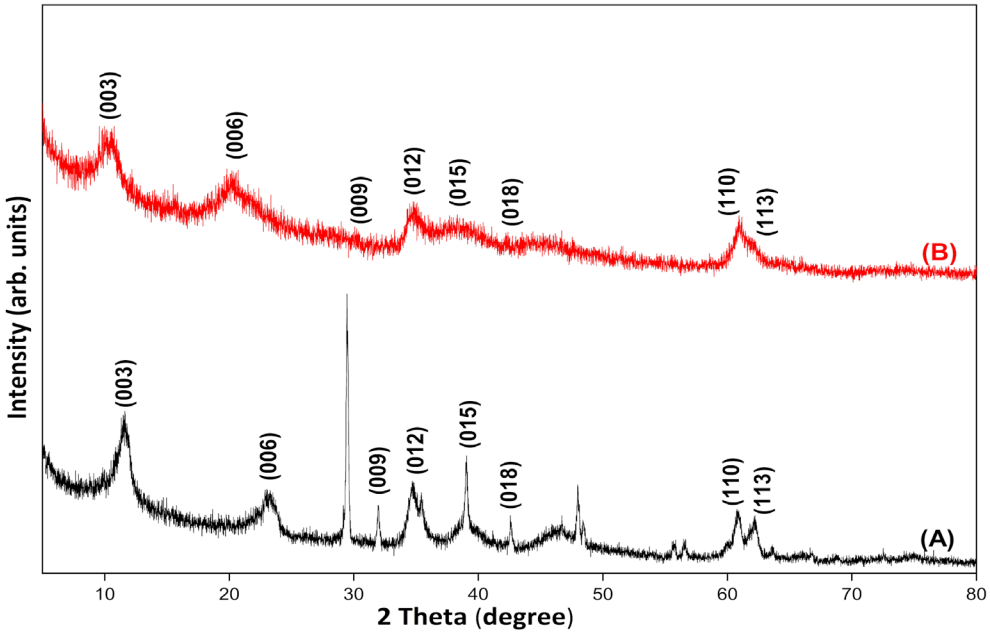

Figure 1. PXRD patterns of (A) Mg-Al LDH (B) WLE-LDH with miller indices of the planes

The typical LDH diffractogram shows three major reflections (usually indexed as (003), (006), and (009)), with (003) being the most significant and appearing around a 2θ value of 10° (Ferencz, 2016). The (003) reflection specific to the LDH structure was visible at a 2θ value of 11.62°. This peak position agreed with that reported for nitrate-intercalated LDH, which showed a sharp diffraction peak at a 2θ value of 11.7° to an index of (003) (Kim et al., 2018). Pristine LDH showed sharp diffraction peaks for (003), (006), (012), (015), (018), (110), and (113). This PXRD pattern of pure nitrate–LDH agreed well with that reported in the literature (Kim et al., 2018, 2019; Jeung et al., 2019). As a result, it was clear that the co-precipitation method had produced Mg-Al LDH, and the reconstruction method had produced WLE-LDH successfully. Furthermore, previous studies showed that after incorporating plant extract into LDH (003), (006), (012), and (110), clear peaks in the PXRD pattern were seen irrespective of the plant extract (Kim et al., 2018, 2019; Jeung et al., 2019). The PXRD pattern of WLE-LDH also showed those four peaks, proving the successful synthesis of WLE-LDH. The diffraction peaks' intensity and sharpness can indicate the quality of the LDHs (Nejati et al., 2016). At lower angles, the pristine LDH exhibited two sharp basal reflections, indexed (003) and (006), and at higher angles, it exhibited two well-separated (110) and (113) diffraction peaks, indicating the generation of a well-crystallized layered structure. According to the literature, there is a relation between the intensity of the (003) reflection and the crystallinity degree of the sample (Nejati et al., 2016). Pristine LDH showed quite remarkable crystallinity in contrast to WLE-LDH and remarkable changes were observed for WLE-LDH. The well-defined diffraction peaks of the Mg-Al LDH were replaced by broad peaks of low intensity. Thus, WLE-LDH showed lower crystallinity. The lower crystallinity of WLE-LDH was thought to be due to random stockpiling of LDH nanosheets and large organic moieties present in the extract, implying the extract incorporation within the LDH nanocomposites. Furthermore, the PXRD patterns provided evidence that structural modifications, particularly those attributed to interlayer distances, occurred following the incorporation of white lotus extract into the layered double hydroxides. Regardless of the lack of new peaks, a peak shift of 0.607° was observed at the basal peak corresponding to the (003) plane in the WLE-LDH nanohybrid. The original d-spacing value of 7.609 Å reported for the pristine LDH of the (003) plane increased to 8.216 Å in the WLE-LDH nanohybrid. This shift of the first-order basal plane reflection of pristine LDH in the direction of higher d-values or lower 2θ values (Table 1) indicates that organic anions present in the flower extract were successfully intercalated into the layered double hydroxides inter lamellar gallery. This increase in the interlayer distance resulted from strong interactions arising between the phytochemicals such as flavonoids, alkaloids, polyphenols of *N. nucifera* Gaertn. flower extract and the hydroxyl layers of LDH and positively charged cations present in the layers of LDH. During the synthesis, the nitrate ions originally present in the LDH were driven out of the layers and the basic pH medium facilitated the formation of negatively charged phytochemical structures. Consequently, white lotus flower extract could move in between the layers of the LDH.

However, because of anionic competition during the synthesis, there was no nitrate intercalation in WLE-LDH, as evidenced by the lack of any peaks originating from the pristine-LDH. The preference for anionic valency during the formation of LDHs could be used to explain the observation. Higher valent anions are typically preferred over lower valent anions because they cause less steric hindrance in the interlayer spaces (Perera et al., 2015). Furthermore, the presence of hydroxyl and carboxylate groups in the bioactive phytochemical anions caused them to form a very strong hydrogen bond network in the interlayer region.

Table 1. 2θ values of the pristine LDH and WLE-LDH

Plane	Pristine LDH (2θ)	d (Å)	WLE-LDH (2θ)	d (Å)	Interlayer distance difference (Å)
003	11.62	7.609	10.76	8.216	0.607
006	23.01	3.862	20.71	4.285	0.423
009	31.94	2.800	30.23	2.954	0.154
012	34.69	2.584	34.49	2.598	0.014
015	39.06	2.304	38.32	2.347	0.043
018	42.57	2.122	42.38	2.131	0.009
110	60.78	1.523	60.93	1.519	-0.004
113	62.22	1.491	61.17	1.514	0.023

The presence of the characteristic peak for (003) in the MgFe-CO_3-LDH PXRD pattern at 11.04° indicated that changes in the trivalent cation and anion had an impact on the 2θ value but that the presence of (003) reflection was unique to the LDH irrespective of the two cations and the anion (Kim et al., 2019). In the literature, the same plant extract incorporated into LDH in two ways evidenced two 2θ values for (003) reflection in PXRD patterns. The 2θ values for the (003) reflection from the ion exchange reaction and reconstruction reaction were 10.60° and 11.38°, respectively (Jeung et al., 2019). This further confirmed that the reconstruction method had successfully produced WLE-LDH, as shown in Figure 1. Moreover, it was previously stated that the reconstruction method demonstrated a more severe crystallinity change than the ion exchange method (Jeung et al., 2019), assisting the lower crystallinity of WLE-LDH synthesized *via* the reconstruction reaction. This finding suggested that the reconstruction method selectively encapsulated plant extract into pristine LDH.

3.3 FTIR of the white lotus flower crude extract, pristine LDH, and WLE-LDH

FTIR spectroscopy data also provided additional conclusive information about the successful intercalation of *N. nucifera* Gaertn. flower extract into the pristine LDH. The intercalated sample IR spectra were comparable to those of the pristine LDH and *N. nucifera* Gaertn. flower extract (Figure 2).

The organic components are present in the *N. nucifera* Gaertn. flowers such as flavonoids, phenols, alkaloids, and saponins contain aromatic rings, carbonyl groups, hydroxyl groups, and aliphatic C-C and C=C bonds in their structure. A peak shift of 5.45 cm^{-1} was observed in the O−H stretching at 3383.88 cm^{-1} in the WLE-LDH followed by peak broadening. The changes were brought about by newly formed H bonds between the hydroxyl groups of *N. nucifera* Gaertn. flower extract phytochemicals, metal hydroxides and interlayer water molecules. The carbonyl stretching peak shifted by 0.95 cm^{-1} to a lower wavelength in the nanohybrid, indicating the reduction of electron density around oxygen atoms due to the formation of H bonds with LDH layers and intermolecular water molecules. Additionally, the peak shifts in the −OH bonding regions of WLE-LDH also support the formation of H bonds. The Mg-O-H stretching peak and Al-O-H stretching peak also showed FTIR peak shifts due to the H bond formation. These metal-oxygen stretching bands are specific in LDH (Nejati et al., 2016).

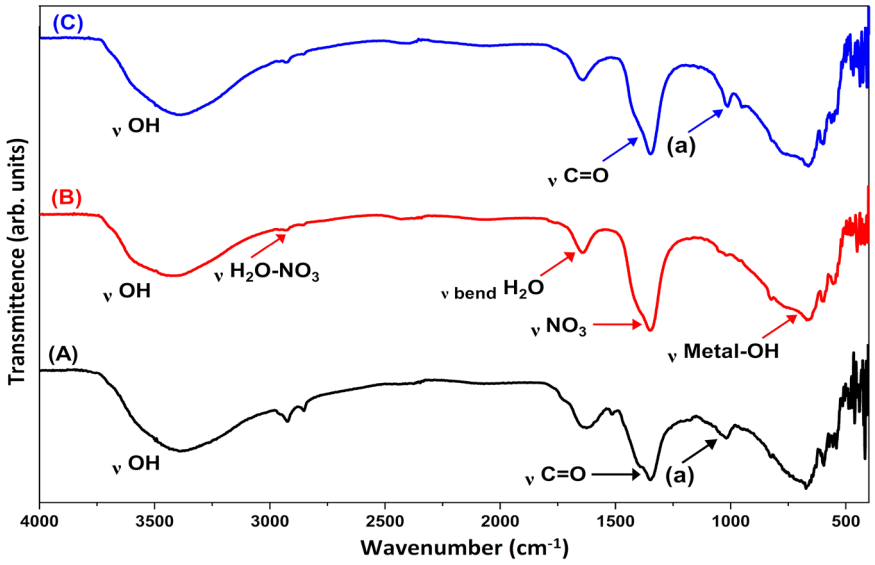

Figure 2. Full FTIR spectra of (A) *N. nucifera* Gaertn. flower extract, (B) Mg-Al LDH, and (C) WLE-LDH

The stretching vibration at around 1015 cm^{-1} (band (a) (Figure 2(A) and 2(C)) is present in both the intercalated sample and the white lotus crude spectra but not in the pristine LDH. This discovery confirms the successful formation of the organic-inorganic nanocomposite. Therefore, the bands in WLE-LDH supported the conclusion that anions of *N. nucifera* Gaertn. flower extract was intercalated into the pristine LDH and were stabilized within the interlayers of the pristine LDH. Figure 2 depicts the IR spectrum of the WLE-LDH hybrid, which included coexisting Metal-OH and O-Metal-O lattice vibrations of the pristine LDH and C=O, aliphatic C-C, C=C, aromatic C-C stretching from the flower extract of *Nelumbo nucifera* Gaertn. These results indicated that after the reconstruction reaction, the intact structures of the phytoconstituents in white lotus flower extract were safely retained in the WLE-LDH hybrid. The assignment of functional groups in FTIR is further illustrated in Table 2.

3.4 SEM images of pristine LDH and WLE-LDH

SEM analysis was used to characterize the size and shape of the LDHs, which were visualized as hexagonal platelets with sharp edges for both pristine LDH and WLE-LDH. Thus, the hexagonal-shaped layered structure, which is typical of LDHs, was observed (Ferencz, 2016; Tang et al., 2018). The SEM images of pristine LDH and WLE-LDH show these characteristics, as depicted in Figure 3(a) and Figure 3(b), respectively. The amorphous phase is thought to be caused by smaller particles adhering to form larger aggregates. The random stacking up of layers of LDHs also can be seen in Figure 3(a) and Figure 3(b) as inter-particle cavities. These inter-particle spaces were expected to be seen in WLE-LDH. It was claimed that the reconstruction reaction has the ability to encase the large biomolecules in natural extracts, giving a morphology that features inter-particle spaces (Jeung et al., 2019). According to the SEM images, this finding was in agreement

Table 2. Major IR peaks of the *Nelumbo nucifera* Gaertn. flower crude extract, pristine LDH, and WLE-LDH

***Nelumbo nucifera* Gaertn. flower crude extract**		**Pristine LDH**		**WLE-LDH**	
Bond mode	**Wavenumber (cm^{-1})**	**Bond mode**	**Wavenumber (cm^{-1})**	**Bond mode**	**Wavenumber (cm^{-1})**
OH stretching	3389.33	OH stretching	3429.92	OH stretching	3383.88
Aliphatic C-C	2924.42	H_2O-NO_3 bridging	2931.42	Aliphatic C-C	2926.31
Aliphatic C-C	2869.00	H_2O bending	1645.58	Aromatic C=C	1638.81
Aromatic C=C	1624.58	NO_3 stretching	1348.51	Aromatic C=C / C-N bond / Carbonyl stretching	1347.40
Aromatic C-C / C-N bond/ Carbonyl stretching	1348.35	Metal-OH lattice vibrations	723.00-517.19	Alcoholic C-O / C-H aromatic	1012.87
Alcoholic C-O / C-H aromatic	1018.95	O-Metal-O lattice vibrations	477.79-404.76	Metal-OH lattice vibrations	662.02
				O-Metal-O lattice vibrations	444.93

with previous study (Kim et al., 2018), in which the primary particle sizes of pristine LDH and WLE-LDH hybrid were comparable. The SEM images further supported the PXRD data by revealing that the LDH's crystallinity decreased once the organic guest molecules were intercalated.

3.5. Release behavior of WLE-LDH

3.5.1 Antioxidant activity

The percentage of *N. nucifera* Gaertn. flower bioactive phytoconstituents intercalated into the lamellar structure was observed to be 80%. The release profile of antioxidant activity studies of WLE-LDH (Figure 4) showed a high initial drug release rate in the first 2 h and 45 min which then reached an almost constant level over a longer period (for about 35 min), confirming the slow, bulk, and sustained release of the drug. The first 1800 s (30 min) showed bulk, fast release of *N. nucifera* Gaertn. flower phytochemicals, indicated by a

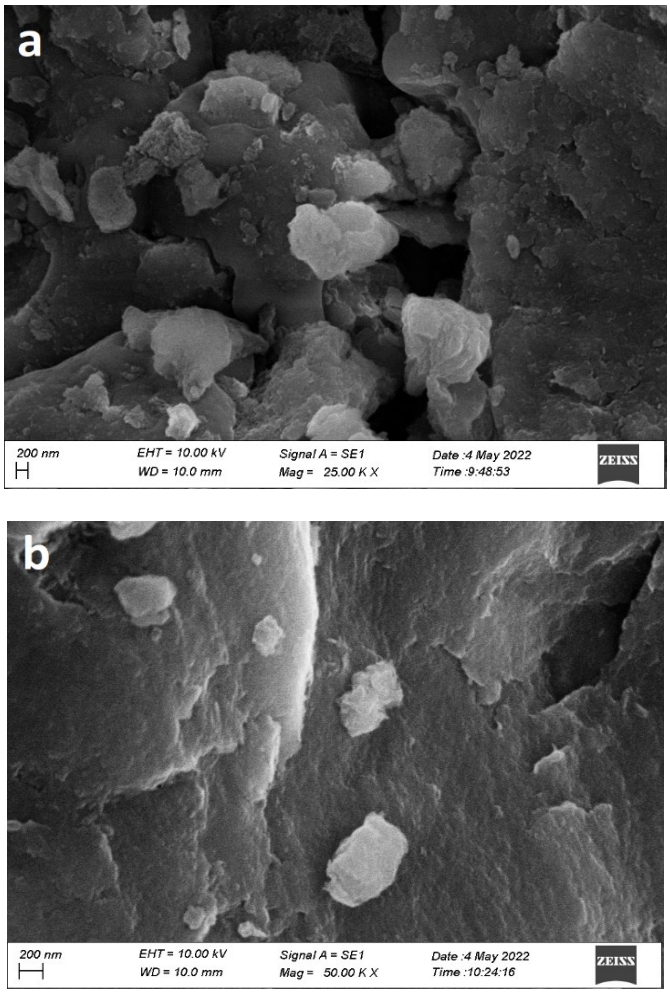

Figure 3. SEM imaging of nanomaterials
(a) Pristine LDH (b) WLE-LDH. Scale bar 200 nm.

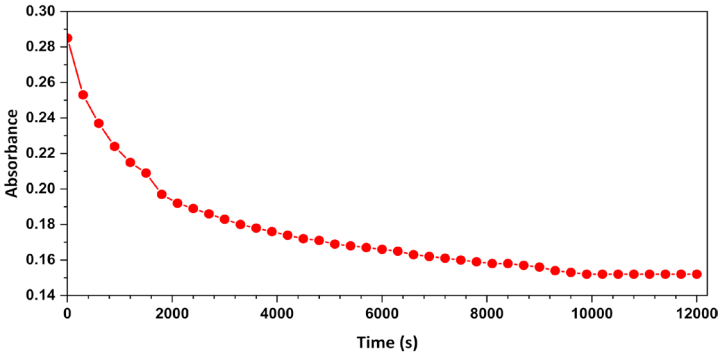

Figure 4. Release profiles of phytochemicals for antioxidant activity from WLE-LDH

steep decrease in absorbance from 0.285 to 0.204. Therefore, within the first 1800 s (30 min) the released lotus extract had an effective reduction of the DPPH radical. Thereafter slow-gradual release up to 9900 s (165 min) resulted in a decrease in absorbance values at a constant rate. The amount of DPPH radical reduction into DPPH-H increased as the amount of lotus extract released from the WLE-LDH increased. The reduction of the DPPH radical by *N. nucifera* Gaertn. flower extract was attributed to this reduction of absorbance values from 0.285 to 0.163, up to 6900 s (115 min). The absorbance value then remained constant, resulting in no further conversion of DPPH radical into reduced DPPH-H form. This could be due to the sustained release of flower extracts from WLE-LDH. This release profile resembles a diffusion-controlled release process (Megalathan et al., 2016). According to the results, 49% of the intercalated phytochemicals were released within the first 1 h for antioxidant activity. The concentration of phytochemicals released from WLE-LDH in 1 h was 0.392 g mL^{-1}.

3.5.2 Anti-tyrosinase activity

The slow sustained release of *N. nucifera* Gaertn. flower extract for anti-tyrosinase activity was shown by release behavioral studies that demonstrated the appropriateness of WLE-LDH nanohybrids as an advanced material for novel skin whitening applications (Figure 5).

The first 1500 s (25 min) showed an increase in absorbance. This demonstrated that the phytochemicals in lotus extract are not attached to the free tyrosinase, allowing L-tyrosine to be converted to dopachrome in subsequent reactions. Then, the decrease in absorbance values evidenced that the lotus phytochemicals from the WLE-LDH bind to the enzyme-substrate complex, not the free enzyme. This confirmed the uncompetitive inhibition of flower extract from the nanohybrid. Furthermore, the released characteristics of the lotus phytochemicals from the WLE-LDH showed a slow-gradual release from 1500 s (25 min) to 6900 s (115 min). The amount of dopachrome formation decreased as the amount of *N. nucifera* Gaertn. extract released from the WLE-LDH increased. The inhibition of tyrosinase by lotus flower extract was attributed to the reduction of absorbance values from 0.500 to 0.465, up to 6900 s (115 min). The absorbance value then remained constant, resulting in the production of a constant amount of dopachrome and no further inhibition of tyrosinase. This revealed the sustained release of the phytochemicals from WLE-LDH. This release profile resembles a diffusion-controlled release process (Megalathan et al., 2016). According to the observed results, 80.63% intercalated phytochemicals was released within the first 1 h. The phytochemical concentration released by WLE-LDH in 1 h was 0.645 g mL^{-1}.

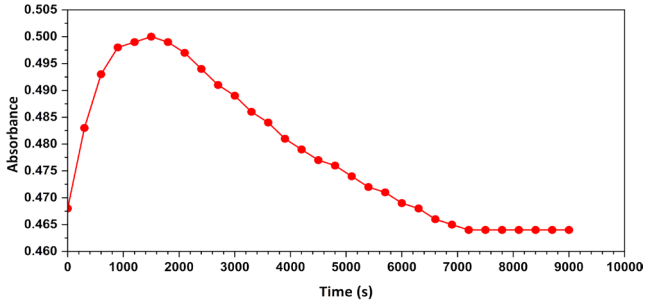

Figure 5. Release profiles of phytochemicals from WLE-LDH for anti-tyrosinase activity

3.6 Photo-stability of WLE-LDH

UV exposure data of the synthesized WLE-LDH nanohybrid was evaluated to establish the photostability of the nanohybrid and to investigate the suitability of the nanohybrid as an antioxidant and anti-tyrosinase agent. The photostability study of *N. nucifera* Gaertn. flower extract was shown by an increase in the absorbance at 520 nm with time of UV exposure (Figure 6(i)). Compared with this, there was only a negligible increase in the absorbance of WLE-LDH (Figure 6(ii)). Therefore, this negligible increase in the absorbance confirmed the protection of the molecules within the LDH layered structure. The phytochemical functional groups in lotus flower extract formed H bonds and electrostatic interactions with LDH layers. Even after prolonged exposure to UV radiation, WLE-LDH maintained flower extract bioactivity while acting as a protective barrier.

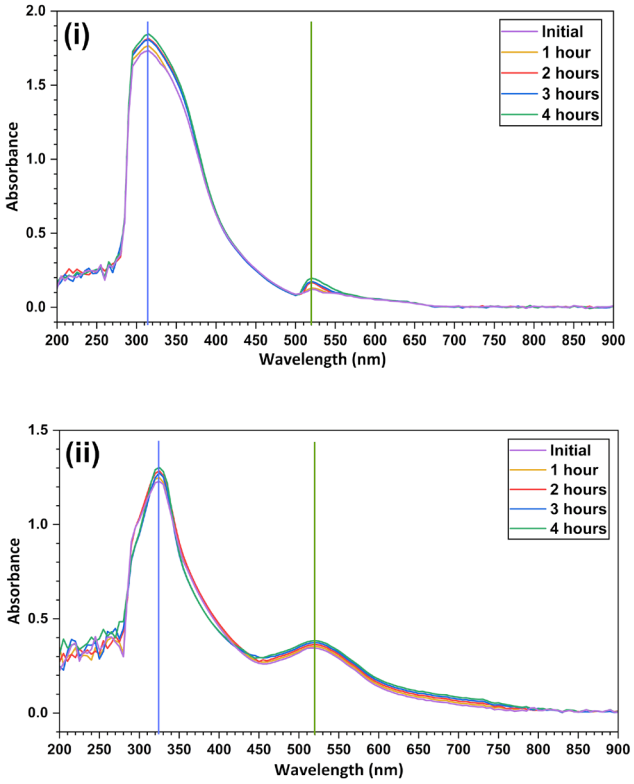

Figure 6. Absorbance spectra of DPPH radical after reduction by (i) *Nelumbo nucifera* Gaertn. flower crude extract and by (ii) WLE-LDH

3.7 DPPH radical scavenging assay of *Nelumbo nucifera* Gaertn. crude extract and WLE-LDH series

The antioxidant activity of WLE-LDH was explored using the DPPH radical scavenging assay. According to the observations, the *N. nucifera* Gaertn. flower extract and WLE-LDH both showed potential antioxidant activity. The reduction of the DPPH radical was

monitored in the assay by measuring the lowering in absorbance at 520 nm wavelength through the reaction. The antioxidant (AH) or radical species reduce DPPH radical into DPPH-H, showing a color change from deep purple to pale yellow (Brand-Williams et al., 1995). Potential antioxidants found in lotus flower extract include flavonoids, alkaloids, phenolic compounds, and polysaccharides (Pandita & Pandita, 2020). Therefore, the hydroxyl groups in those chemical constituents donate hydrogen to the DPPH radical, reducing it to the DPPH-H reduced form. The results showed that as the extract concentration increased, the amount of hydrogen donor molecules present in the flower extract solution increased. Thus, *Nelumbo nucifera* Gaertn. flower extract showed dose-dependent potent antioxidant activity. The organic anions present in the lotus flower extract, which have potent antioxidant activity, were intercalated within the metal hydroxide layers of pristine LDH. As a result, the WLE-LDH solution series exhibited an inhibition percentage variation ranging from 0.00% to 63.11% (Table 3). As a result, the number of bioactive molecules released from the bilayers increased as the WLE-LDH concentration increased.

Table 3. Inhibition percentage of WLE-LDH solution series for antioxidant activity and for anti-tyrosinase activity

Concentration (mg mL^{-1})	Inhibition percentage (%)	
	Antioxidant activity	Anti-tyrosinase activity
0.00	0.00	0.00
0.0625	15.05	1.44
0.125	27.18	4.03
0.25	33.17	25.63
0.5	47.41	44.64
1.0	63.11	64.64

The total extract of *N. nucifera* Gaertn. flowers showed dose-dependent antioxidant activity with a half-maximum effective concentration (EC_{50}) value at a concentration of 0.17 mg mL^{-1} (Figure 7(i)) while the WLE-LDH showed antioxidant activity with a EC_{50} value at a concentration of 0.58 mg mL^{-1} (Figure 7(ii)). The standard (L-ascorbic acid) has an EC_{50} value at a concentration of 0.04 mg mL^{-1} (Figure 7(iii)). In this context, the lotus flower extract exhibited high antioxidant activity with a low EC_{50} value of 0.17 mg mL^{-1}, whereas the WLE-LDH exhibited efficient antioxidant activity with a slightly high EC_{50} value of 0.58 mg mL^{-1} compared to the L-ascorbic acid. Unlike the lotus flower extract, in WLE-LDH, the amount of lotus flower crude extract intercalated within the bilayers was 80 wt% and the antioxidant effect happened *via* those released bioactive molecules from the pristine LDH bilayers. Therefore, a somewhat high concentration of WLE-LDH solution was required to produce 50% of the maximum effect compared to the lotus flower extract which was not intercalated between any bilayer.

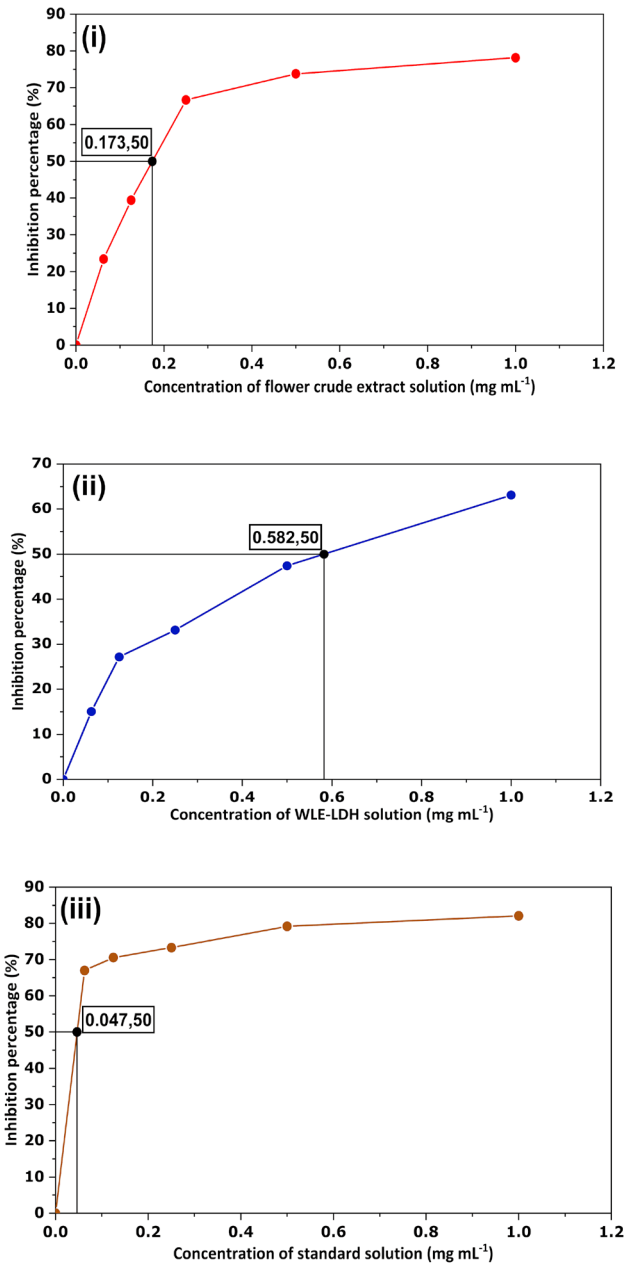

Figure 7. Inhibition percentage VS concentration plots for antioxidant activity for the series of (i) *N. nucifera* Gaertn. flower crude samples, (ii) WLE-LDH solutions, and (iii) standard solutions

3.8 Anti-tyrosinase enzyme assay of *Nelumbo nucifera* Gaertn. crude extract and WLE-LDH series

The anti-tyrosinase activity of WLE-LDH was tested using tyrosinase enzyme assay. According to the findings, both the *N. nucifera* Gaertn. flower extract and WLE-LDH showed potent anti-tyrosinase activity. In the presence of atmospheric oxygen, tyrosinase first catalyzes the hydroxylation of tyrosine to form dihydroxyphenylalanine (DOPA). After that, tyrosinase further catalyzes the conversion of DOPA to dopaquinone, which then spontaneously converts to dopachrome which gives a dark red color. The dopachrome eventually turns into a black pigment called melanin. This whole process is referred to as the melanin biosynthesis pathway. The red-colored compound, dopachrome, showed an absorbance peak at 475 nm (Venier, 2015). Therefore, the formation of dopachrome was monitored in the assay by measuring the lowering in absorbance at wavelength of 475 nm through the reaction. The results demonstrate that as the extract concentration increased, the amount of dopachrome formed decreased, meaning that the lotus flower extract acted as an enzyme inhibitor in the enzyme assay. This was supported by the evidence that flavonoids, phenols, and alkaloids found in lotus flowers extract could have anti-tyrosinase activity (Noysang & Boonmatit, 2019; Wu et al., 2019). Similarly, the WLE-LDH solution series demonstrated potent anti-tyrosinase activity. The anti-tyrosinase activity of the WLE-LDH solution series and the flower crude extract solution series was nearly identical (graph pattern in Figure 8 (i) and (ii)). Negatively charged organic molecules in *N. nucifera* Gaertn. flower extract with potent anti-tyrosinase activity had intercalated within the metal hydroxide layers of pristine LDH. It was only the released bioactive constituents from the metal hydroxide layers that caused the WLE-LDH solution series to display varying inhibition percentage from 0.00% to 64.64% (Table 3). As a result, the number of bioactive molecules released from the bilayers increased as the WLE-LDH concentration increased. According to our results, the proper concentration of the WLE-LDH for anti-tyrosinase activity was 1.0 mg mL^{-1}, which showed higher inhibition percentage 64.64% (Table 3).

The *N. nucifera* flower extract showed dose-dependent anti-tyrosinase activity with a half maximum inhibitory concentration (IC_{50}) value at a concentration of 0.43 mg mL^{-1} (Figure 8(i)), while the WLE-LDH showed anti-tyrosinase activity with a IC_{50} value at a concentration of 0.63 mg mL^{-1} (Figure 8(ii)). The standard had an IC_{50} value at a concentration of 0.37 mg mL^{-1} (Figure 8(iii)). Concluding that the *N. nucifera* Gaertn. flower extract had strong anti-tyrosinase activity with a low IC_{50}, whereas WLE-LDH had a potent anti-tyrosinase activity with a slightly higher IC_{50} value comparable to the standard, arbutin.

3.9 Enzyme kinetic study for *Nelumbo nucifera* Gaertn. flower crude extract solution

In the final series of studies, we examined the enzyme kinetics of the enzyme inhibitor, *N. nucifera* Gaertn. flower extract. In the control, both K_M and V_{max} values were higher compared to the values in the presence of an enzyme inhibitor (Table 4).

In the presence of the flower extract (1/V), values were higher compared to the values in the control (Table 5). The Lineweaver-Burke plots displayed different slopes and intercepts in the presence of enzyme inhibitor (Figure 9(a)) and the control (Figure 9(b)). Additionally, K_M and V_{max} both decreased in the presence of lotus flower extract (Figure 9c). Thus, the type of inhibition of *N. nucifera* Gaertn. flower extract was determined as an

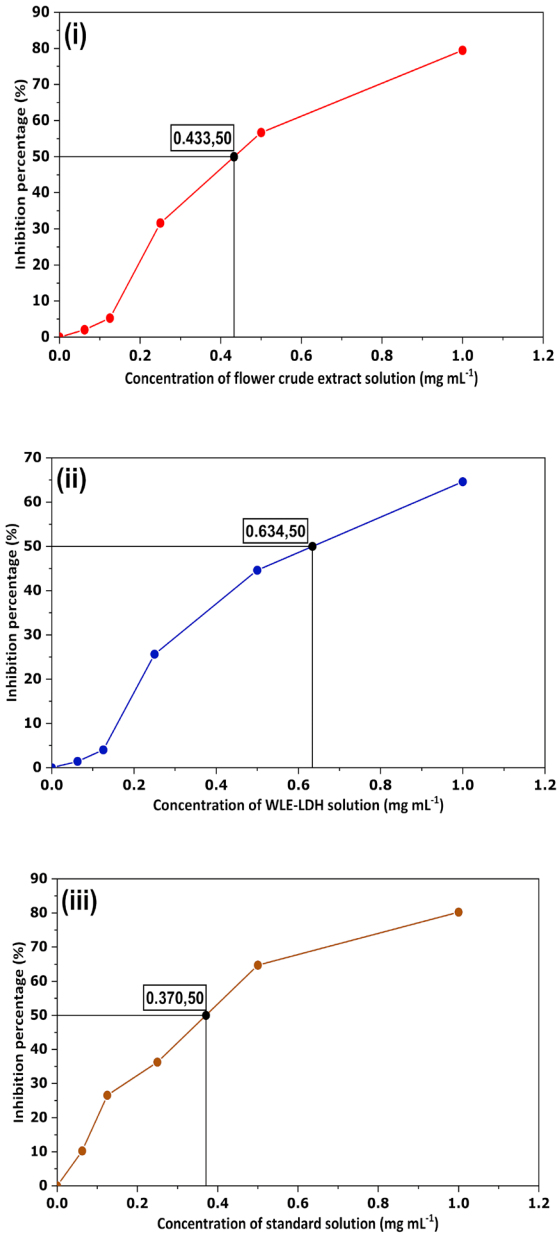

Figure 8. Inhibition percentage VS concentration plots for anti-tyrosinase activity for the series of (i) *N. nucifera* Gaertn. flower crude samples, (ii) WLE-LDH solutions, and (iii) standard solutions.

Table 4. Kinetic parameters in the absence and presence of lotus flower extract

Entry	K_M (mM)	Vmax ($\Delta A_{475\ nm}$/s)
In the absence of the flower extract (control)	16.99	55.72×10^{-5}
In the presence of the flower extract	1.38	6.04×10^{-5}

Table 5. Results of 1/[S] and (1/V) in the absence and presence of lotus flower extract

Entry	1/[S] (mM^{-1})	1/V ($(\Delta A_{475\ nm}/s)^{-1}$)	
		In the presence of the flower extract	In the absence of the flower extract (control)
1	2	59880.2395	59880.2935
2	1	42918.4549	37453.1835
3	0.67	37453.1835	27247.9564
4	0.5	30030.0300	15797.7883
5	0.4	21413.2762	12500.0000
6	0.33	20000.0000	7315.28895

uncompetitive inhibitor. Uncompetitive inhibition is a special situation where the inhibitor cannot bind directly to the enzyme, but only to the enzyme-substrate complex (ES). Therefore, once L-tyrosine binds to the active sites of the enzyme and forms the enzyme-substrate complex, the extract can attach to the ES and prevent further reactions from occurring. Furthermore, L-tyrosine is converted to L-DOPA, and when that L-DOPA binds to the enzyme and forms ES, the lotus extract may also inhibit the subsequent reactions. This discovery could be related to the first part of the release study of anti-tyrosinase activity, which revealed an increase in absorbance values. The increase in absorbance values imply the released extract itself could not bind to the enzyme but once ES was formed, it could bind. As a result of the slow release of extract from the WLE-LDH and the uncompetitive inhibition of *N. nucifera* Gaertn. extract, the absorbance values increased in the first 25 min (Figure 5).

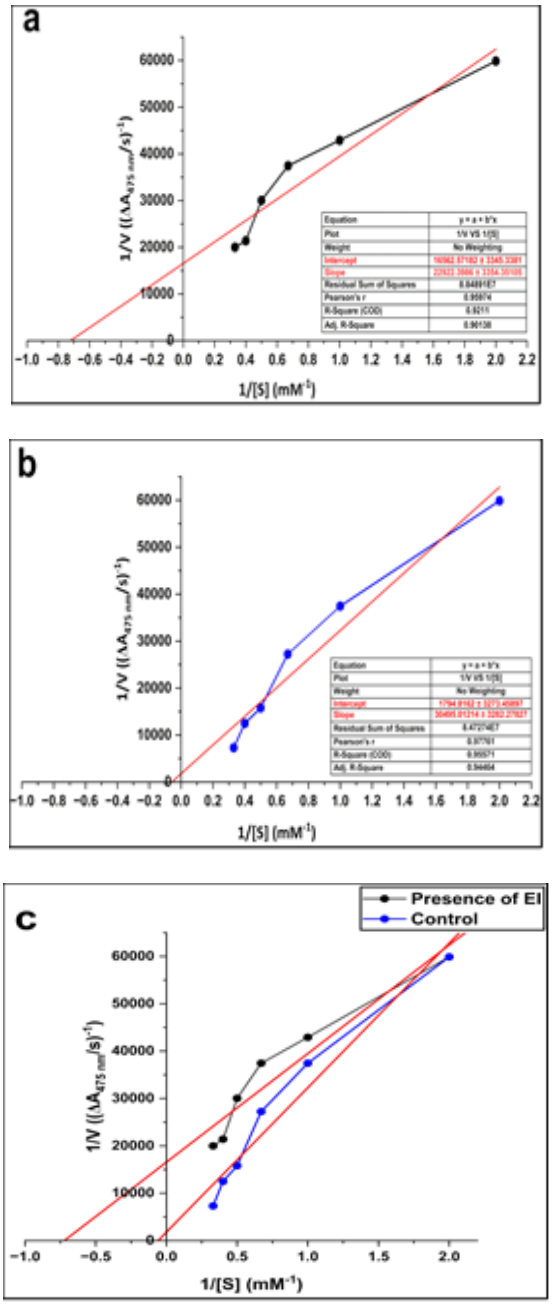

Figure 9. Lineweaver-Burke plots, (a) in the presence of *N. nucifera* Gaertn. flower extract, (b) in the absence of *N. nucifera* Gaertn. flower extract, (c) the comparison of two Lineweaver-Burke plots which are in the presence (black) and absence (blue) of *N. nucifera* Gaertn. flower extract.

4. Conclusions

The main goal of this study was to prepare layered double hydroxide (LDH) encapsulated *Nelumbo nucifera* Gaertn. flower extract (WLE-LDH) and examine the antioxidant and anti-tyrosinase capacities of the WLE-LDH. To help with drug delivery and application, we also investigated the release behavior and photo-stability of the *N. nucifera* Gaertn. flower extract encapsulated LDH. In summary, we demonstrated the first successful encapsulation of the *N. nucifera* Gaertn. flower extract into pristine LDH *via* the reconstruction method. PXRD and FTIR data confirmed the successful encapsulation of the flower extract into pristine LDH. Moreover, SEM images of the flower extract encapsulated LDH (WLE-LDH) revealed typical hexagonal platelet morphology with layered structures. According to quantitative analysis, 80 wt% of the crude extract was incorporated into the LDH. The WLE-LDH displayed remarkable antioxidant activity with maximum inhibition percentage of 63.11% and anti-tyrosinase activity with maximum inhibition percentage of 64.64% compared to the standards. Furthermore, the flower extract encapsulated LDH demonstrated slow and sustained release characteristics proving its applicability in skin whitening formulations. When the photo-stability of WLE-LDH was investigated, the encapsulated product demonstrated UV stability for 4 h. The enzyme kinetics data of *N. nucifera* Gaertn. flower extract matched the WLE-LDH release profile, implying that the action mechanism was based on flower extract bioactive constituent dissolution from the pristine LDH bilayers. Based on these superior features, we believe that these *N. nucifera* Gaertn. flower extracts incorporated into layered double hydroxide nanocomposites are suitable for developing novel topical skin applications as they can function as efficient drug delivery systems.

5. Acknowledgements

We gratefully acknowledge the financial support from the Department of Chemistry, University of Colombo, Sri Lanka, the CAMD laboratory at the Department of Chemistry, University of Colombo, Sri Lanka for providing PXRD facility, University of Moratuwa, Sri Lanka for providing SEM facility, and Techno Solutions Pvt. Ltd, Nugegoda, Sri Lanka for providing FTIR facility.

6. Conflicts of Interest

The authors declare no conflicts of interest.

ORCID

Jayani C. Dhanasinghe https://orcid.org/0009-0009-7165-294X

Nadun S. Ubeysinghe https://orcid.org/ 0009-0002-0455-7511

Ireshika C. De Silva https://orcid.org/0000-0001-6793-3612

References

Alcântara, A. C. S., Aranda, P., Darder, M., & Ruiz-Hitzky, E. (2010). Bionanocomposites based on alginate-zein/layered double hydroxide materials as drug delivery systems. *Journal of Materials Chemistry*, 20(42), 9495-9504. https://doi.org/10.1039/c0jm01211d

Ashraf, Z., Rafiq, M., Seo, S. Y., Kwon, K. S., Babar, M. M., & Zaidi, N. U. S. S. (2015). Kinetic and in silico studies of novel hydroxy-based thymol analogues as inhibitors of mushroom tyrosinase. *European Journal of Medicinal Chemistry*, *98*, 203-211. https://doi.org/10.1016/j.ejmech.2015.05.031

Bakhouche, I., Aliat, T., Boubellouta, T., Gali, L., Şen, A., & Bellik, Y. (2021). Phenolic contents and in vitro antioxidant, anti-tyrosinase, and anti-inflammatory effects of leaves and roots extracts of the halophyte Limonium delicatulum. *South African Journal of Botany*, 139, 42-49. https://doi.org/10.1016/j.sajb.2021.01.030

Brand-Williams, W., Cuvelier, M. E., & Berset, C. (1995). Use of a free radical method to evaluate antioxidant activity. *LWT - Food Science and Technology*, 28(1), 25-30. https://doi.org/10.1016/S0023-6438(95)80008-5

Chen, J., Ran, M., Wang, M., Liu, X., Liu, S., Ruan, Z., & Jin, N. (2021). Evaluation of antityrosinase activity and mechanism, antioxidation, and UV filter properties of theaflavin. *Biotechnology and Applied Biochemistry*, 69(3), 951-962. https://doi.org/10.1002/bab.2166

Crespo, M. I., Chabán, M. F., Lanza, P. A., Joray, M. B., Palacios, S. M., Vera, D. M. A., & Carpinella, M. C. (2019). Inhibitory effects of compounds isolated from Lepechinia meyenii on tyrosinase. *Food and Chemical Toxicology*, 125, 383-391. https://doi.org/10.1016/j.fct.2019.01.019

Daniel, S. & Thomas, S. (2020). Layered double hydroxides: fundamentals to applications. In S. Thomas & S. Daniel (Eds.), *Layered double hydroxide polymer nanocomposites* (pp. 1-76). Woodhead Publishing.

Dubey, S., & Baghel, S. S. (2019). Phytochemical investigation and determination of phytoconstituents in flower extract of Nelumbo nucifera. *Journal of Drug Delivery and Therapeutics*, 9(1), 146-149. https://doi.org/10.22270/jddt.v9i1.2197

Eckelt, R., Olfs, H., Kosslick, H., & Torres-Dorante, L. (2009). Comparison of different synthesis routes for Mg–Al layered double hydroxides (LDH): Characterization of the structural phases and anion exchange properties. *Applied Clay Science*, 43, 459-464.

Ferencz, Z. (2016). *Mechanochemical preparation and structural characterization of layered double hydroxides and their amino acid-intercalated derivatives*. [Doctoral dissertation, University of Szeged]. SZTE Doktori Repozitórium Archive. https://doktori.bibl.u-szeged.hu/id/eprint/2886/8/tezisfuzet_angol.pdf

Gunawardana, S. L. A., & Jayasuriya, W. J. A. B. N. (2019). Medicinally important herbal flowers in sri lanka. *Evidence-Based Complementary and Alternative Medicine*, 2019, Article 2321961. https://doi.org/10.1155/2019/2321961

Jeon, S., Kim, N. H., Koo, B. S., Kim, J. Y., & Lee, A. Y. (2009). Lotus (*Nelumbo nuficera*) flower essential oil increased melanogenesis in normal human melanocytes. *Experimental and Molecular Medicine*, 41(7), 517-524. https://doi.org/10.3858/emm.2009.41.7.057

Jeung, D.-G., Kim, H.-J., & Oh, J.-M. (2019). Incorporation of *Glycine max Merrill* extract into layered double hydroxide through ion-exchange and reconstruction. *Nanomaterials*, 9(9), Article 1262. https://doi.org/10.3390/nano9091262

Karunaratne, V., Kottegoda, N., & de Alwis, A. (2012). Nanotechnology in a world out of balance. *Journal of the National Science Foundation of Sri Lanka*, 40(1), 3-8. https://doi.org/10.4038/jnsfsr.v40i1.4165

Kim, H.-J., Lee, S.-B., Choi, A.-J., & Oh, J.-M. (2019). *Zingiber officinale* extract (ZOE) incorporated with layered double hydroxide hybrid through reconstruction to preserve antioxidant activity of ZOE against ultrasound and microwave irradiation. *Nanomaterials*, 9(9), Article 1281. https://doi.org/10.3390/nano9091281

Kim, H.-J., Lee, G. J., Choi, A.-J., Kim, T.-H., Kim, T.-I., & Oh, J.-M. (2018). Layered double hydroxide nanomaterials encapsulating *Angelica gigas* nakai extract for potential

anticancer nanomedicine. *Frontiers in Pharmacology*, 9, Article 723. https://doi.org/10.3389/fphar.2018.00723

Kim, T. H., Kim, H. J., Choi, A. J., Choi, H. J., & Oh, J. M. (2016). Hybridization between natural extract of angelica gigas nakai and inorganic nanomaterial of layered double hydroxide via reconstruction reaction. *Journal of Nanoscience and Nanotechnology*, 16(1), 1138-1145. https://doi.org/10.1166/jnn.2016.10688

Kim, T., Kim, H. J., Cho, S. K., Kang, W. Y., Baek, H., Jeon, H. Y., Kim, B., & Kim, D. (2011). Nelumbo nucifera extracts as whitening and anti-wrinkle cosmetic agent. *Korean Journal of Chemical Engineering*, 28(2), 424-427. https://doi.org/10.1007/s11814-010-0357-6

Liyanaararchchi, G. D., Samarasekera, J. K. R. R., Mahanama, K. R. R., & Hemalal, K. D. P. (2018). *T*yrosinase, elastase, hyaluronidase, inhibitory and antioxidant activity of Sri Lankan medicinal plants for novel cosmeceuticals. *Industrial Crops and Products*, 111, 597-605. https://doi.org/10.1016/j.indcrop.2017.11.019

Megalathan, A., Kumarage, S., Dilhari, A., Weerasekera, M. M., Samarasinghe, S., & Kottegoda, N. (2016). Natural curcuminoids encapsulated in layered double hydroxides: A novel antimicrobial nanohybrid. *Chemistry Central Journal*, 10(1), Article 35. https://doi.org/10.1186/S13065-016-0179-7

Mukherjee, P. K., Mukherjee, D., Maji, A. K., Rai, S., & Heinrich, M. (2009). The sacred lotus (Nelumbo nucifera) - phytochemical and therapeutic profile. *Journal of Pharmacy and Pharmacology*, 61(4), 407-422.

Nejati, K., Mokhtari, A., Khodam, F., & Rezvani, Z. (2016). Syntheses of Mg – Al – NO 3 layered double hydroxides with high crystallinity in the presence of amines. *Canadian Journal of Chemistry*, 94(3), 66-71. https://doi.org/10.1139/cjc-2015-0265

Noysang, C., & Boonmatit, N. (2019). Preliminary phytochemicals and pharmacologic activities assessment of white and pink *Nelumbo nucifera* Gaertn. flowers. *Applied Mechanics and Materials*, 891, 41-51.

Pandita, A., & Pandita, D. (2020). Antioxidants in vegetables and nuts - Properties and health benefits. In G. A. Nayik & A. Gull (Eds.). *Lotus (Nelumbo nucifera Gaertn)*. Springer Nature. https://doi.org/10.1007/978-981-15-7470-2

Perera, J., Weerasekera, M., & Kottegoda, N. (2015). Slow release anti-fungal skin formulations based on citric acid intercalated layered double hydroxides nanohybrids. *Chemistry Central Journal*, 9, Article 27. https://doi.org/10.1186/s13065-015-0106-3

Perotti, G. F., Silva, F. F., de Couto, R. A. A., Lima, F. C. D. A., Petrilli, H. M., Leroux, F., Ferreira, A. M. C., & Constantino, V. R. L. (2020). Intercalation of Apocarotenoids from Annatto (*Bixa orellana* L.) into layered double hydroxides. *Journal of the Brazilian Chemical Society*, 31(11), 2211-2223.

Poellmann, H., & Witzke, T. (2010). *ICDD Grant-in-Aid*. University of Halle, Department of Mineralogy and Geochemistry, Halle/Saale, Germany.

Samindra, K. M. S., & Kottegoda, N. (2014). Encapsulation of curcumin into layered double hydroxides. *Nanotechnology Reviews*, 3(6), 579-589. https://doi.org/10.1515/ntrev-2014-0018

Sasidharan, S., Chen, Y., Saravanan, D., Sundram, K. M., & Yoga Latha, L. (2011). Extraction, isolation and characterization of bioactive compounds from plants' extracts. *African Journal of Tradititional Complementary and Alternative Medicine*, 8(1), 1-10.

Shafiei, S. S., Solati-Hashjin, M., Samadikuchaksaraei, A., Kalantarinejad, R., Asadi-Eydivand, M., & Osman, N. A. A. (2015). Epigallocatechin gallate/layered double hydroxide nanohybrids: Preparation, characterization, and in vitro anti-tumor study. *PLoS One*, 10(8), Article e136530. https://doi.org/10.1371/journal.pone.0136530

Srichayanurak, C., & Phadungkit, M. (2008). Antityrosinase and antioxidant activities of selected thai herbal extracts. *KKU Research Journal*, 13(6), 673-676.

Subasini, U., Thenmozhi, S., Venkateswaran, V., Pavani, P., Diwedi, S., & Rajamanickam, G. V. (2014). Phytochemical analysis and anti hyperlipidemic activity of nelumbo nucifera in male wistar rats. *International Journal of Pharmacy Teaching and Practices*, 5(1), 935-940.

Tang, L. P., Cheng, H. M., Cui, S. M., Wang, X. R., Song, L. Y., Zhou, W., & Li, S. J. (2018). DL-mandelic acid intercalated Zn-Al layered double hydroxide: A novel antimicrobial layered material. *Colloids and Surfaces B: Biointerfaces*, 165, 111-117. https://doi.org/10.1016/j.colsurfb.2018.02.017

Tettey, C. O., Nagajyothi, P. C., Lee, S. E., Ocloo, A., Minh An, T. N., Sreekanth, T. V. M., & Lee, K. D. (2012). Anti-melanoma, tyrosinase inhibitory and anti-microbial activities of gold nanoparticles synthesized from aqueous leaf extracts of *Teraxacum officinale*. *International Journal of Cosmetic Science*, 34(2), 150-154. https://doi.org/10.1111/j.1468-2494.2011.00694.x

Tringali, C. (2001). *Bioactive compounds from natural sources*. Taylor & Francis.

Venier. (2015). Enzyme analysis using tyrosinase. In Venier (Ed.), *Advanced biology with Venier* (2nd ed., pp. 283-290). Vernier software and technology.

Wu, J., Xu, J. G., Fu, J. P., Xiong, W., Zhang, S. W., Gu, Z., Wu, L., & Hu, J. W. (2019). Characterization of tyrosinase inhibitors from white lotus receptacle. *Chemistry of Natural Compounds*, 55(5), 929-931. https://doi.org/10.1007/s10600-019-02849-7